

Field and Laboratory Study of the Mn/DOT Precast Slab Span System

Matthew Smith
Department of Civil Engineering
University of Minnesota
500 Pillsbury Drive SE
Minneapolis, MN 55455
smit1475@umn.edu

Carol Shield
Department of Civil Engineering
University of Minnesota
500 Pillsbury Drive SE
Minneapolis, MN 55455
ckshield@umn.edu

Whitney Eriksson
Department of Civil Engineering
University of Minnesota
500 Pillsbury Drive SE
Minneapolis, MN 55455
erik0065@umn.edu

Catherine French
Department of Civil Engineering
University of Minnesota
500 Pillsbury Drive SE
Minneapolis, MN 55455
cfrench@umn.edu

ABSTRACT

The Minnesota Department of Transportation (Mn/DOT) Precast Slab Span System was initially designed by Mn/DOT with input from University of Minnesota researchers and local fabricators. The bridge system consisted of a series of precast, prestressed concrete inverted tee bridge elements which also served as stay-in-place formwork for the cast-in-place portion of the deck placed in the field. One of the Mn/DOT implementations, located in Center City, MN, was instrumented. The bridge has been monitored for reflective cracking and continuity over the piers since the deck was cast. Transverse load distribution was evaluated with a static truck test. In addition, a two-span test specimen was constructed to investigate effects of variations in flange thickness, bursting reinforcement, horizontal shear reinforcement, and flange surface treatment. The data obtained from the field study indicated that cracking had initiated in the bridge at the locations of some of the gages at midspan and near the support. The cracking was determined to be the result of environmental loads and shrinkage rather than due to vehicular loads. The data from the truck tests indicated that the design assumption of a monolithic slab system was valid for the determination of load distribution factors. The results of the laboratory study showed that positive restraint moments developed in the precast system for which continuity was made at a young age (i.e., seven days), and that these moments could be reasonably well predicted by existing models. It has also been found that current American Association of State Highway and Transportation Officials bursting requirements require unnecessary transverse reinforcement in the end zones of slab span systems.

Key words: bursting reinforcement—composite—precast—restraint moment—slab span

PROBLEM STATEMENT

The need to accommodate increasing volumes of traffic while replacing the aging infrastructure has resulted in a need to implement new construction techniques. Quality control, safety issues, and environmental concerns associated with onsite concrete casting, have prompted wider acceptance for the use of precast elements. Rural areas, where many short to intermediate span bridges are located, have additional motivation for precast construction due to limited specialty contractors for post-tensioning and formwork. A team of engineers who participated in a 2004 Federal Highway Administration International Scanning Tour of Prefabricated Bridge Elements and Systems identified a number of systems considered for implementation. A variation of the precast Poutre Dalle slab span system, originally developed in France, has been implemented by the Minnesota Department of Transportation (Mn/DOT). The goal of this research was to better understand the performance of the system to improve design guidelines and develop standard details.

RESEARCH OBJECTIVES AND METHODOLOGY

The Mn/DOT Precast Slab Span System was initially designed by Mn/DOT with input from the University of Minnesota (U of MN) researchers and local fabricators. The bridge system consisted of a series of precast prestressed concrete inverted tee bridge elements which also served as stay-in-place formwork for the cast-in-place (CIP) portion of the deck placed in the field. A typical cross section is shown in Figure 1, where precast depths of 12 to 16 in. have been used for spans ranging from 22 to 45 ft. One of the Mn/DOT implementations located in Center City, MN was instrumented by the U of MN researchers. The bridge has been monitored for reflective cracking and continuity over the piers since the deck was cast September 19, 2005. Transverse load distribution was evaluated with a static truck test.

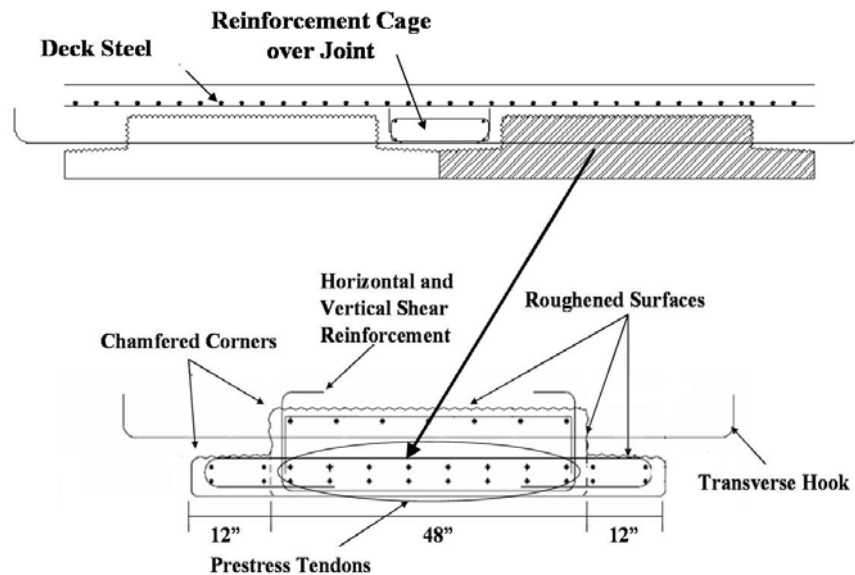


Figure 1. Conceptual cross section of Mn/DOT Precast Slab Span System

In addition, a two-span test specimen was constructed in the U of MN Structures Laboratory to investigate effects of variations in flange thickness, bursting reinforcement, horizontal shear reinforcement, and flange surface treatment. Each span employed two precast panels that incorporated combinations of these parameters. One of the four precast sections was identical to those used in the Center City Bridge. The precast inverted tee beams were cast September 6, 2006, and the CIP deck was

cast seven days later to maximize the positive restraint moment that develops in precast systems made continuous by a CIP deck. The restraint moment was monitored for 250 days after the continuity pour.

Implementation considerations for the Mn/DOT Precast Slab Span System included the potential for development of reflective cracking that may occur due to stress concentrations between flanges of adjacent precast sections and over web corners of individual precast sections, and design issues such as restraint moments, bursting reinforcement requirements, continuity over the pier and load distribution factors.

RESTRAINT MOMENT

When bridge systems are made continuous with a CIP deck, restraint moments need to be considered which develop as a result of variations in time-dependent effects between the precast and CIP elements. As part of the laboratory study, the two-span test bridge was monitored for restraint moment development. These results were compared to the original design calculations and methods found in the literature (Freyermuth 1969; Peterman and Ramirez 1998). The design considerations of NCHRP 519, which have been incorporated in American Association of State Highway and Transportation Officials (AASHTO) LRFD 2007, were also investigated.

Methodology of Restraint Moment Study

As mentioned above, the CIP deck was cast on relatively young (seven-day-old) precast inverted tees to maximize the effects of the positive restraint moments over the pier. Because younger precast beams will have increasingly similar shrinkage development as the CIP deck, the creep due to prestress dominates the behavior and greater positive moments are developed. The differential age of seven days was chosen as a reasonable minimum for practical construction limitations. Positive restraint moments negate to some degree the benefit of continuous bridge construction as the positive midspan moment is increased. These moments are difficult to address in design because positive moment connections with capacities beyond $1.2M_{cr}$, where M_{cr} is the cracking moment of the diaphragm, are not efficient as they may increase the positive restraint moment by attracting more moment. Consequently, it is recommended that steps be taken to reduce the positive moment if necessary (Miller et al. 2004).

The development of restraint moments was monitored by placing load cells under the supports of the ends of the laboratory specimen. Equilibrium was used to calculate the corresponding restraint moments using the center of bearing length shown in Figure 2.

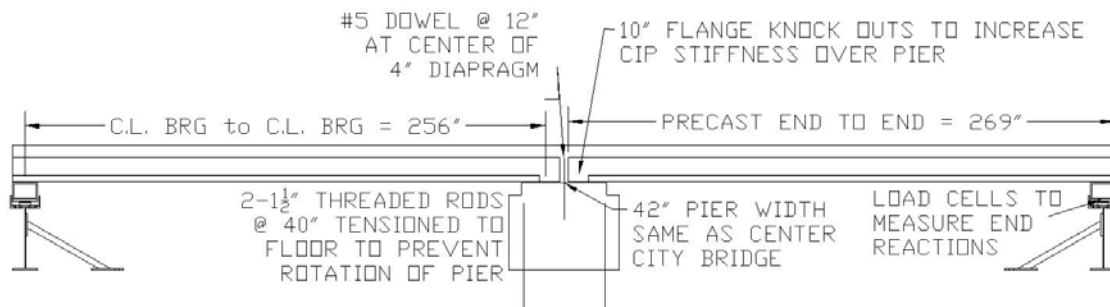


Figure 2. Elevation of laboratory specimen

Key Findings

Results from the laboratory study were compared to the Portland Cement Association (PCA) Method (Freyermuth 1969) and the P-Method (Peterman and Ramirez 1998). The primary differences between these methods were the modeling assumptions at the pier and the values assumed for creep and shrinkage. In the P-Method, the diaphragm is modeled as a small span between the bearing supports of adjacent beams, whereas the PCA Method uses a single support at the center of the pier. For the Center City Bridge, the P-Method predicted restraint moments 14% larger than the PCA Method due to the modeling assumption at the piers. For creep and shrinkage, the PCA Method provides charts from which values were scaled. The P-Method provides no creep and shrinkage values, so AASHTO LRFD (2004) Section 5.4.2.3 was used. The creep and shrinkage values from the PCA Method were much higher than those from the AASHTO LRFD. Using the laboratory specimen as an example, the values assumed for maximum differential shrinkage and the ultimate creep coefficient were of 135 $\mu\epsilon$ and 2.66, respectively, for the PCA Method and 88 $\mu\epsilon$ and 1.01, respectively, for the AASHTO LRFD. The change in strain at the center of gravity of the strands in the web of each of the four precast sections in the laboratory specimen has been monitored since the beams were cast and shows better agreement to the combined creep and shrinkage predicted by the models in AASHTO LRFD (2004) than the PCA Method as shown in Figure 3. For the models, Young's modulus was calculated using AASHTO LRFD (2004) C5.4.2.4-1 using the precast and CIP 28 day strengths of 12.9 ksi and 4.3 ksi, respectively. Other required parameters included the age at prestress transfer (1 day), the cure time for the precast beams (1 day) and CIP deck (8 days), and the average measured relative humidity (40%).

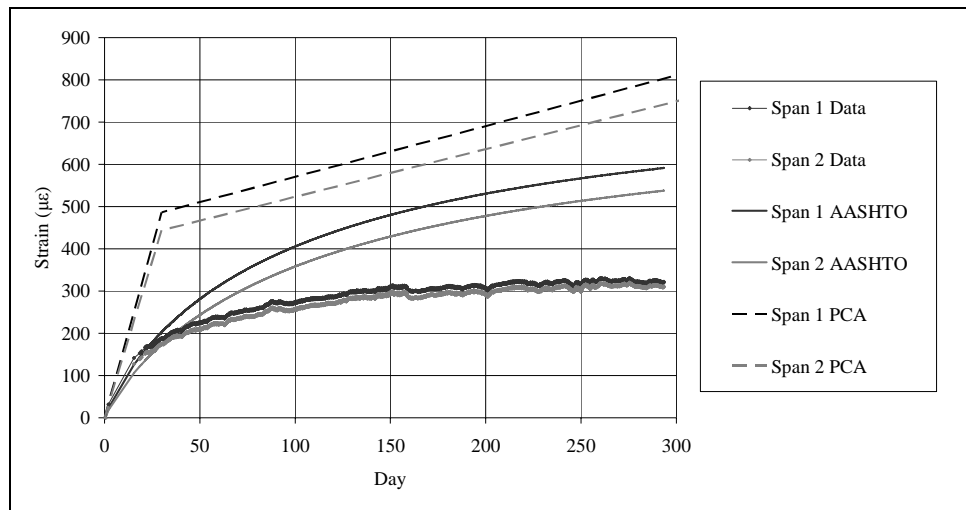


Figure 3. Combined creep and shrinkage strains from center of gravity of prestress strands

The two methods were also applied to two of the Mn/DOT Slab Span bridges, assuming continuity at 14 and 90 days, which predicted positive and negative restraint moments, respectively. In these cases, the PCA method was found to predict slightly smaller positive restraint moments and much larger negative restraint moments than the P-Method as shown in Table 1. The main reason for the difference in negative restraint moment between the methods was a factor to account for the shrinkage restraint due to the longitudinal stiffness of the deck steel and precast section that was used in the P-Method but not in the PCA Method. Creep of the precast and differential shrinkage predictions were both higher for the PCA Method for continuity at 14 days, but the resultant was similar to the P-Method prediction. For the Center City Bridge, the shrinkage restraint factor reduced free shrinkage by 64% and 70%, respectively, using design and measured strengths to calculate relative stiffnesses. Stiffnesses were calculated using AASHTO LRFD C5.4.2.4-1 where the design strengths were 6.5 and 4.0 ksi for the precast beams and

CIP deck, respectively, and the measured 28 day strengths from the laboratory specimen were 12.9 and 4.3ksi for the precast beams and CIP deck, respectively. The PCA method has been found to over-predict negative restraint moments in other studies as well (Peterman and Ramirez 1998; Miller et al. 2004).

Table 1. Predicted restraint moments for Mn/DOT Slab Span bridges (ft.-kips)

| | Positive restraint moment (Continuity at 14 days) (Predicted at 20 years after continuity) | | Negative restraint moment (Continuity at 90 days) (Predicted at 100 days after continuity) | |
|--|--|-------------|--|------------|
| | PCA Method | P-Method | PCA Method | P-Method |
| | Center City Bridge 04002 | 78.5 142 | 106 149 | 198 266 |

The AASHTO LRFD (2004) Section 5.14.12.2.7c requirement for considering a fully effective continuous joint was found to be extremely restrictive for the Center City Bridge. This provision essentially required the positive restraint moment to be smaller than the sum of the superimposed dead load moment and one half the live load moment. Because the span lengths for the Center City Bridge were only 22, 27, and 22 ft., the applied moments were small, and the positive restraint moment was limited to only 71 ft-kips or $0.46M_{cr}$. This appeared too conservative, and it seems reasonable to limit the positive restraint moment to the cracking moment of the diaphragm. However, because the cracking moment may be over predicted due to insufficient bond at the ends of the precast sections, a reduction factor may be required.

Figure 4 shows the calculated restraint moments for the P-Method and PCA Method using measured material and geometrical parameters for each span of the laboratory specimen, with the creep and shrinkage models for the respective methods described above. The predictions obtained from the PCA Method were piecewise linear due to the limited data points for creep over time; whereas the P-Method results were obtained using a daily time step. Cross sections for both spans are given in Figure 5. The predicted strand stresses in the 16 web strands of each precast section immediately after transfer were used as the prestress force in the restraint moment calculations, and they were 194 and 195 ksi, respectively for Spans 1 and 2 using measured properties. The strands in the flange were neglected because they were only nominally stressed. A line at $0.6M_{cr}$, half the recommended limit from NCHRP 519, is shown for scale. The P-Method predicted different restraint moments for the two spans that reflect the design changes in the specimen (e.g., reduction in precast concrete area). There was not a similar change for the PCA method because the modeling assumption of a single roller support at the pier resulted in a single value for the restraint moment at the pier that combined the effects of the two spans. The data from the west span is missing from the 14th to the 161st day due to an error in monitoring setup. The daily fluctuations in the data were due to temperature changes which became more pronounced towards the end of the monitoring period when work related to other projects began requiring the doors to the structures laboratory to be opened.

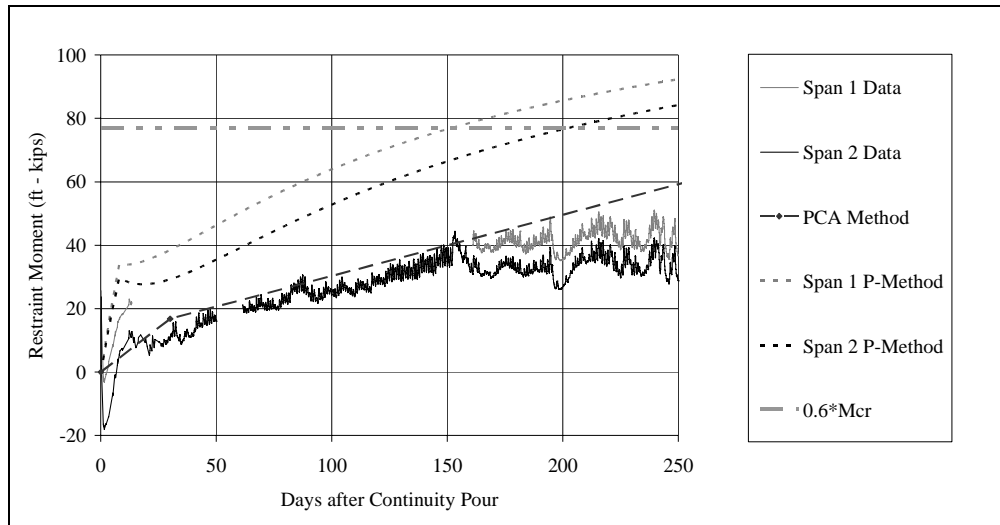


Figure 4. Restraint moments from laboratory specimen

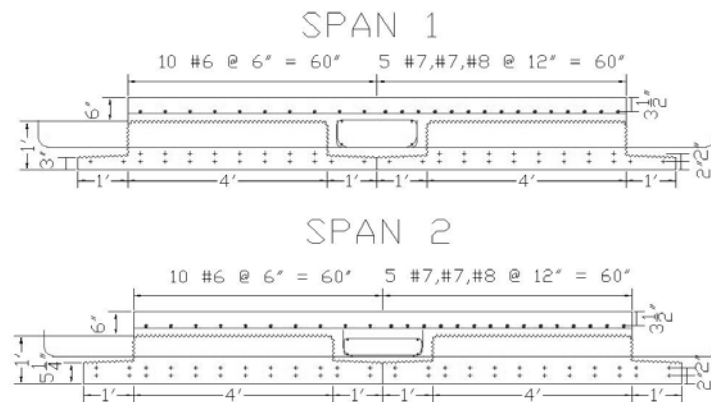


Figure 5. Laboratory specimen cross sections

The measured data were expected to be less than the predictions because the models assumed roller(s) at the pier where in reality the pier support should have behaved as a rotational spring as can be seen in the pier connection in Figure 2. The negative restraint moment developed over the first several days was likely due to the cooling of the CIP deck after casting which is not considered by either of the models, and this consideration would allow for an upward shift in the measured results to an unknown degree. Considering the high degree of uncertainty due to the variability of material properties and imperfect modeling assumptions, both methods provided reasonable estimates of the positive restraint moment developed over the first 250 days. But this was somewhat of a coincidence as competing differences within the models canceled out. For example, when the time of continuity was changed from 7 to 28 days, the P-Method predicted restraint moments of -3 and 63 ft-kips at 30 days and 20 years after continuity, respectively, whereas the PCA Method predicted -182 and 17 ft-kips, for the same time frames. In these cases, the differences in the predictions would greatly affect both positive and negative moment design at the pier. Although the PCA Method appeared to provide a better estimate of the restraint moment, the creep and shrinkage results from the laboratory specimen in Figure 3 show that the PCA Method over predicted the strains that drove positive restraint moment development. In contrast, the P-Method predictions had similar relations to the measured data in both Figures 3 and 4, which infers that the shrinkage restraint factor, and creep and shrinkage models assumed for the P-Method provided a better model of the behavior than the PCA Method. Without the large creep coefficient predicted from the PCA

Method, there would not have been enough positive restraint moment from prestress creep to counter the large negative restraint moment due to the assumption of unrestrained shrinkage.

Figure 6 shows the two models carried out to the 20-year service life of the bridge. It is unknown whether the positive restraint moment would have reached 120 ft-kips as it appeared to have tapered off closer to 40 ft-kips. This is consistent with the readings of the strain gages at the center of gravity of the strand shown in Figure 3, where the creep and shrinkage strains in the precast sections that drove positive moment development leveled off compared to either of the model predictions.

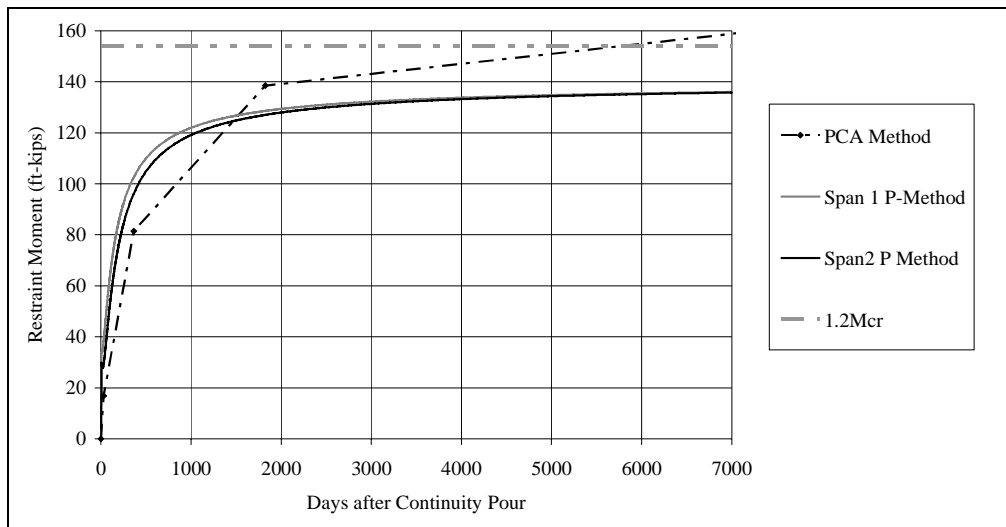


Figure 6. Laboratory specimen predictions carried out to 20 years

BURSTING

Horizontal cracks frequently form in the end zone of prestressed members when the prestress force is transferred to the concrete. These cracks, known as bursting cracks, result from vertical tension created by the transfer of forces from the prestressing strand to the concrete. If unrestrained, these cracks can extend into the member and decrease strength and durability. Previous studies have determined these cracks cannot be eliminated, but vertical reinforcing steel can limit crack widths and propagation (Fountain 1963). AASHTO's 1961 Interim Specifications introduced a minimum vertical reinforcement requirement for the end zones of pretensioned members, which has since remained almost unchanged. Meanwhile, pretensioning use has increased along with developments in cross section shape, higher strength materials, and increased strand sizes allowing for greater prestressing forces within members. Despite these advances, AASHTO has not made significant modifications to bursting steel requirements. The purpose of this investigation is to determine if the current AASHTO bursting requirements are applicable to the precast slab span system.

Development of AASHTO Bursting Requirements

The 1961 Interim AASHTO Specifications introduced bursting requirements for I-beams stating, "Vertical stirrups acting at 20,000 psi to resist 4% of the prestressing force shall be placed within $d/4$ from the end of the beam with the end stirrup placed as close to end of beam as practicable," where d is the effective depth. By 1969 the above requirements were made applicable to end zones of all prestress beams, not just I-beams. The only difference between the 1969 provisions and the current, 2007 AASHTO LRFD Bridge Design Specifications is that vertical steel can now be placed within $h/4$ from the

end face, where h is the member height, instead of $d/4$. It is generally assumed the original AASHTO provisions were developed as a result of experimental testing performed on I-beams by Marshall and Mattock (1962). This suggests the original AASHTO requirements, developed for I-beam members, are not necessarily applicable to other cross sections, particularly slab span systems.

The current AASHTO bursting provisions can require a large amount of vertical steel to fit in a small area. For slab span systems and other sections small in height, fitting the required vertical steel within one quarter of the height from the end face causes congestion and complicates prestressing strand and concrete placement. For the laboratory slab span specimen, with a height of 12 in., all bursting steel was required to fit within 3 in. from the end. Allowing 2 in. for clear cover, only 1 in. was available for bursting steel placement, which was not feasible.

Marshall and Mattock (1962) used experimental tests on I-beams to develop a design equation for the area of bursting steel necessary to limit bursting crack width and propagation. The first series of tests were conducted on ten 22.5 in. tall I-beams with no vertical tension steel. Members varied by strand configuration, web thickness and strand surface condition. Maximum tensile strains were found to occur on the end face near mid-depth. The strains decreased quickly from the end face to reach zero at a distance no further than one-quarter of the height from the end face. The second series of tests were conducted on 25 I-beams of 22.5 and 25 in. heights with two sizes of vertical steel. These beams varied by strand size and location and magnitude of prestress force. Results indicated the total vertical reinforcement force was proportional to the prestressing force and inversely proportional to strand transfer length. Using this relationship and experimental data, a design equation was developed for the area of vertical steel needed to limit crack width and propagation.

$$A_s = 0.021 \frac{P}{f_s} \frac{h}{L_t}, \text{ if } \frac{h}{L_t} \leq 2 \quad (1)$$

where T is the total prestress force (kip), h is the height of the section (in.), L_t is the transfer length (in.), and f_s is the allowable working stress of the transverse reinforcement (ksi).

Equation 1 was developed for members with non-uniformly spaced strands in the top and bottom of the member. The AASHTO requirements are equal to the above equation, if h/L_t is set equal to 2.

In an attempt to better quantify the location and magnitude of bursting forces, authors have used finite element models (Gens et al. 2005), equilibrium analyses (Gergely et al. 1963), and strut and tie models (Castrodale et al. 2002). In the Gergely and Sozen (1963) approach, equilibrium analysis was applied to the end zone of a section. In the model, cracking was assumed to occur along the end face at the height of maximum moment. The crack was conservatively assumed to extend a length equal to the height of the member. A free body diagram of the section below the crack is shown in Figure 7. To put the free body into equilibrium, a moment was applied at the top of the free body. This moment was used to determine the tensile force along the face of the member. Although originally developed for post-tensioned systems, this theory is also applicable for pretensioned systems. In a study performed at the University of Nebraska-Lincoln (Tadros et al. 2003), the Gergely-Sozen model was compared to experimental results from Marshall and Mattock's study on pretensioned I-beams. The Gergely-Sozen method was shown to provide a conservative estimate of vertical tensile force in nearly all cases, and ranged between 0.95 and 3.58 times the experimental result.

Table 2 provides a comparison of the different predicted tensile forces from AASHTO (2007), the Marshall and Mattock equation, and the Gergely-Sozen model. These are compared to the experimental

results gathered from literature for an I-beam (Marshall et al. 1962), inverted tee (Tadros et al. 2003) and the laboratory specimen. Note the large difference between experimental values and AASHTO values. A 2003 study on pretensioned systems found that changing AASHTO specifications by decreasing the required tension force to be resisted by the reinforcement from 4% to 3% of the total pretension force would still be conservative (Tadros et al. 2003).

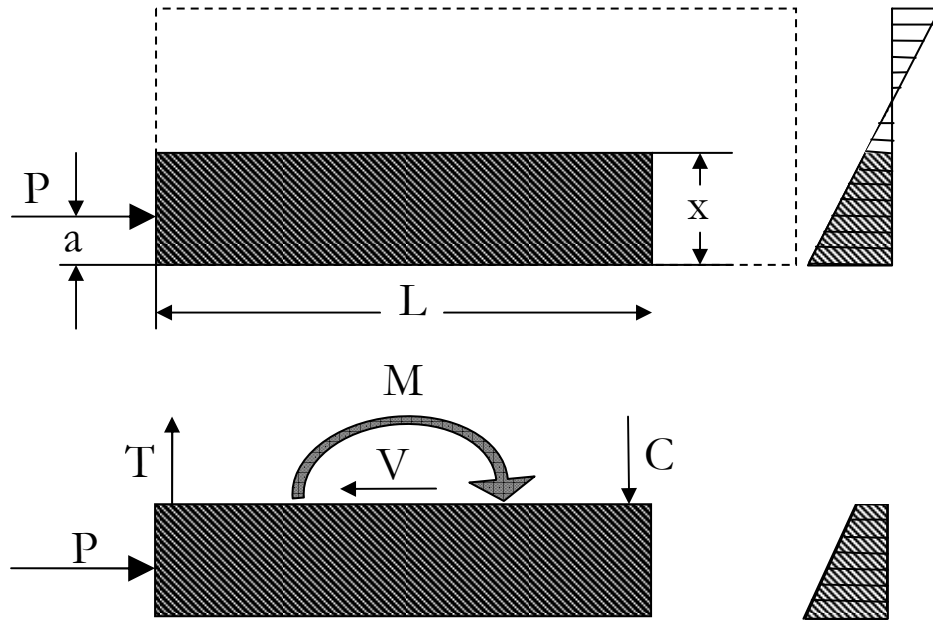


Figure 7. Gergely-Sozen Model (Gergely et al. 1963)

Table 2. Comparison of Predicted Tension Force to Experimental Tension Force Results (kips)

| | AASHTO | Marshall and Mattock | Gergely - Sozen | Experimental |
|---------------------|--------|----------------------|-----------------|--------------|
| I-beam | 11.6 | 12.2 | 11.2 | 5.2 |
| Inverted Tee | 19.8 | 9.8 | 20.8 | 12.2* |
| Laboratory Specimen | 19.8 | 5.0 | 1.6 | 0.0 |

*Average vertical tensile force from 3 studies on identical inverted tee specimens. Results ranged from 10.3 kip to 14.5 kip (Tadros et al. 2003).

Methodology of Bursting Study

Both ends of each precast section for the laboratory specimen were instrumented with steel and concrete strain gages to measure strain in the section. Rosettes were used on the side face of each section, located at mid-height, two in. into the section. Two strain gages were attached to each vertical stirrup placed in the end zones. Four different vertical steel configurations were used for the four precast beams, as shown in Table 3. Two of the configurations used less than half of the area of steel required by AASHTO (2007), and the sections that met the required area of bursting reinforcement were not able to meet the placement requirements (i.e., extended further than three in. from the end into the section).

Table 3. Bursting Steel Configurations for Laboratory Specimen

| | Slab 1 | | Slab 2 | | Slab 3 | | Slab 4 | | AASHTO |
|--|--------|----|--------|----|--------|--------|--------|----|--------|
| Stirrup Location (in. into beam) | 2 | 4 | 2 | 4 | 2 | 4 | 2 | 4 | |
| Vertical Stirrup Size | #3 | #3 | #4 | -- | 2 - #5 | 2 - #5 | #5 | #5 | |
| Total Stirrup Area (in. ²) | 0.44 | | 0.40 | | 2.48 | | 1.24 | | 0.99 |

Key Findings

In the laboratory specimen, the concrete and steel strain gages were monitored at transfer. The measured strains were negligible, and there were no visible signs of cracking. The concrete had adequate strength to resist tensile stresses induced at the time of transfer. Therefore, the quantity of vertical reinforcement in the end zone did not affect the results. Further investigation is being performed to develop recommended changes for bursting requirements.

FIELD BRIDGE STUDY

Methodology of Field Bridge Study

The Center City Bridge was monitored to investigate the effects of environmental and vehicular loads since the deck was cast September 19, 2005. The focus was to watch for the development of reflective cracking. In the center span, three joints were instrumented at midspan as shown in the inset of Figure 8 to monitor the transverse strains over the joint between the precast sections, over the web corners, and in the mild reinforcement that crossed above the joint between the precast sections. In addition, gages were placed on longitudinal mild reinforcement as shown in Figure 8. Load distribution, continuity over the piers, and effects of live load on reflective cracking were investigated by performing static truck tests April 18, 2007. Results were compared to a simple finite element model.

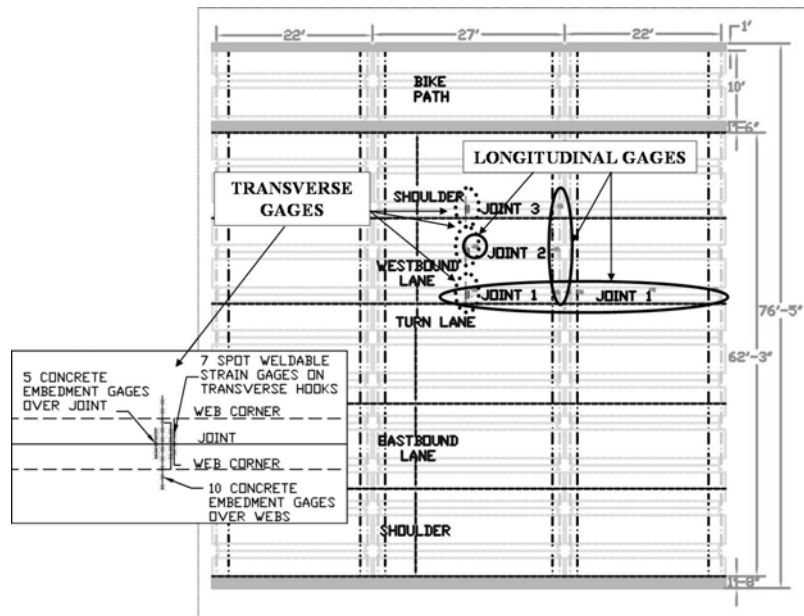


Figure 8. Layout of Center City Bridge

Key Findings

Results from monitoring the bridge for 21 months showed satisfactory behavior. There were, however, sufficient strain readings in two of the three monitored joints and over the pier that indicated some cracking had occurred. Daily strain fluctuations of 165 and 260 $\mu\epsilon$ in the transverse direction at midspan of the middle span in Joints 1 and 3, respectively, were observed. The readings from the adjacent mild reinforcement fluctuated as well, indicating that it was effectively spanning the crack. Stresses in the mild steel reduced along the reinforcement away from the maximum over the joint between the precast sections indicating that the crack was centered on the joint. The absence of similar behavior in the embedment gages above the web corners indicated that the crack had not propagated to that level, although there were visible longitudinal shrinkage cracks on the deck that ran the entire length of the bridge. At the pier, strain readings indicated a positive moment crack. Daily strain changes of greater than 700 $\mu\epsilon$ were recorded on the mild steel of the positive moment connection at mid-depth of the section. As with the transverse cracking, there was no unusual activity observed in the instrumentation directly above indicating that cracking had not propagated to the top of the CIP. The cracking appeared to be driven by the thermal gradient due to the top of the bridge absorbing solar radiation. This caused the bridge to camber, which generated positive restraint moments. All of the activity appeared to have begun abruptly on April 23, 2006. Because the pier developed a positive moment crack, it is unlikely that this was caused by a vehicular load, and, moreover, it is unlikely that a truck could have caused the crack at the pier as indicated by the small strains observed during the truck test. The cracking was most likely due to a combination of shrinkage and temperature effects that reached a critical level.

The truck test performed on April 18, 2007 confirmed that Joints 1 and 3 had reduced stiffness, likely due to cracking. A wheel load placed directly above the joint caused transverse strains of 19 and 32 $\mu\epsilon$, respectively, in the concrete embedment gages immediately above Joints 1 and 3, compared to 8 $\mu\epsilon$ in Joint 2, which had not indicated any cracking. These small strain readings also show how small the effects of vehicular loads were compared to environmental loads. A truck would require an axle weight of more than 60 tons to generate the same transverse strains that temperature effects caused on any given day. Reflective cracking over the web corners was also a concern for the system, but no load position caused a tensile stress in the embedment gages over any of the three monitored joints.

The truck test was also used to evaluate the load distribution factor used by Mn/DOT to design the Center City Bridge. Because none of the categories in AASHTO LRFD 4.6.6.2 directly addressed the Mn/DOT Precast Slab Span System, the equation for effective width of a monolithic concrete slab-type bridge given in AASHTO LRFD (2004) 4.6.2.3 was used for design. Due to the gap between flanges of adjacent precast sections, a reduction in transverse stiffness may cause the effective width to be smaller than that of a monolithic system. Load distribution was evaluated by loading the center span at midspan with a single truck at six locations across the width of the bridge. Midspan curvatures were calculated using gages welded to longitudinal reinforcement in Joints 1 and 2. Figure 9 shows the truck layout for one of these six positions. For the midspan tests, the truck faced west, but the front axle load was neglected since it was near the pier.

Curvatures were calculated by fitting a line through the strains from gages 9 in, 12.5 in, and 15.5 in from the bottom of the 18 in. composite section. Results for the six tests are shown in Figure 10 along with the results of a finite element model of an isotropic flat plate with a smeared stiffness calculated by combining the stiffnesses of the precast sections, CIP deck, and mild deck reinforcement and assuming no cracking. The same stiffness calculations, based on the 28-day strengths of the laboratory specimen components, discussed in the restraint moment findings were used to calculate the smeared isotropic stiffness as it was assumed that the bridge components would have similar stiffnesses to that of the laboratory specimen since the precast sections were made with the same mix from the same precast plant

and both deck mixes followed the Mn/DOT 3Y33 specification. The parapets were included in the model, but only had an effect on the results close to the parapet which allowed for the superposition of the data for the six tests onto a single plot. In the model, the boundary condition at the pier was assumed to be a single roller at the center of the pier. The midspan curvature of the center span corresponding to the same load assumed to be carried over the effective width from the AASHTO equation is also given.

The results generally followed the trend of the isotropic model, from which it can be observed that a design equation for a monolithic slab system is a valid assumption for this system. It can be assumed that longer spans would behave similarly because they will have a deeper overall section, and the height of the gap at the flange tips will be unchanged, so longer span bridges should behave more like monolithic systems than shorter ones. The isotropic model was also used to predict strains near the pier in the middle span where another series of gages was located when the bridge was loaded at midspan. Because the gages were within one depth of the bearing, the assumption of beam theory was not valid, but the strains in the deck steel were compared to those predicted in the isotropic model at the same depths as the gages. The results for both the positive and negative reinforcement are both given in Figure 11. The model predicted negligible strain for the positive moment steel because it was located at mid-depth of the 18 in. composite section (i.e. neutral axis in the model). Again, the results generally followed the trend of the isotropic model, except that the data appeared to be slightly less distributed, but the assumption of a monolithic system appeared to be reasonable. It can also be seen that the strains in the positive moment reinforcement at mid-depth were compressive, which corroborates the existence of positive moment cracking at the pier as the concrete below mid depth must have a reduced stiffness.

Continuity over the pier was also evaluated by analyzing the truck test data from instrumentation in Joint 1. When the center span was loaded at midspan, the midspan deck steel strain in the adjacent span due to negative bending was $1.2 \mu\epsilon$ for a single truck and $1.5 \mu\epsilon$ for two trucks, compared to 1.9 and $3.7 \mu\epsilon$ as predicted by the isotropic model. The loads in these tests were centered on Joint 1 to maximize the results. The discrepancies were most likely due to moment transferred into the substructure at the piers and abutments of the bridge where perfect rollers were assumed in the model. Because the midspan curvatures from the truck test were smaller than those predicted by the isotropic model, the assumption of full continuity appeared to be conservative so long as the benefit of the moment connections at the abutments and piers was ignored. The midspan curvature for the case without continuity at the pier was also plotted in Figure 10 to confirm that the continuity assumption was valid.

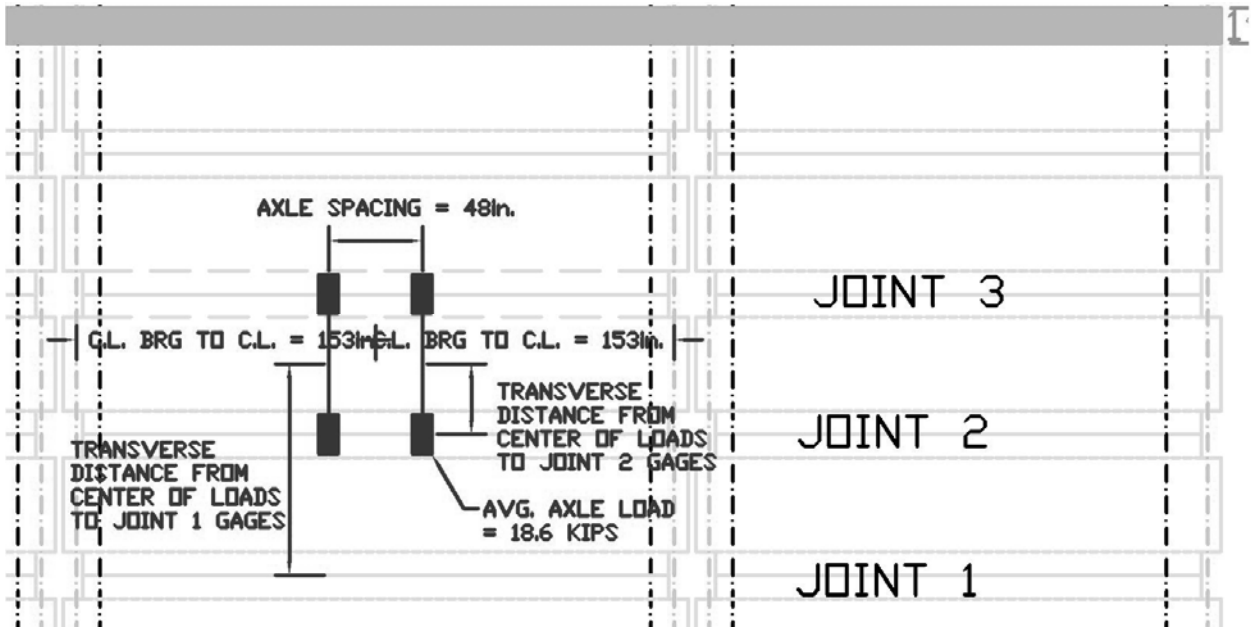


Figure 9. Typical truck test position layout

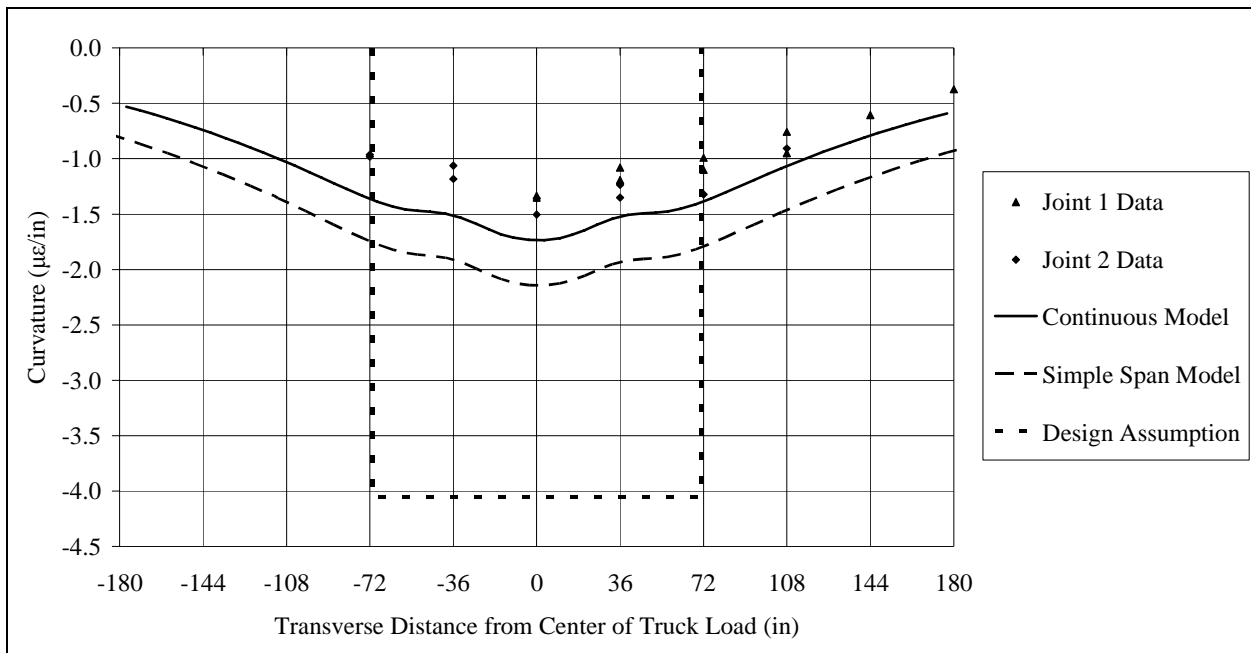


Figure 10. Curvatures at midspan due to a single truck

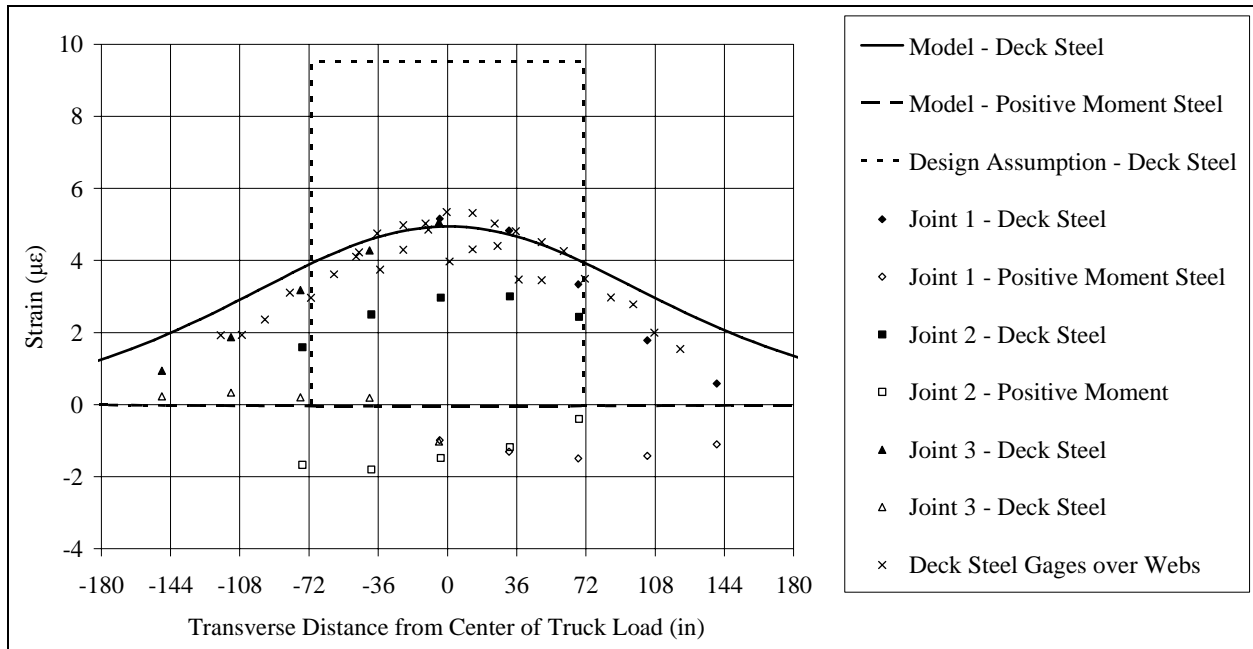


Figure 11. Strains near pier due to a single truck

CONCLUSIONS

The results of the laboratory study showed that both the PCA Method and P-Method provided a reasonable prediction of positive restraint moment development. The creep and shrinkage values were better predicted by AASHTO LRFD (2004) 5.4.2.3 than the charts provided with the PCA Method, and with the absence of the large creep strains predicted by PCA Method to offset the unrestrained shrinkage, the assumption of shrinkage restraint appears to be valid. It has also been found that current AASHTO bursting requirements do not take into account cross section shape and require unnecessary transverse reinforcement in end zones of slab span systems.

The results of the first 21 months of the field study showed that no reflective cracks have propagated above the web corners, and all of the strain fluctuations observed appeared to be initiated and driven by environmental loads and shrinkage. The results from the truck test showed that wheel loading immediately above the joint resulted in strains less than 20% of those observed from environmental loads, even in joints where cracking had been observed. The isotropic plate model reasonably predicted the load distribution of the Center City Bridge due to vehicular loads from which it can be inferred that the assumption of using a monolithic slab system to determine the load distribution factors for design was valid. The assumption of full continuity appeared to be valid so long as the benefit of the moment connections at the abutments and piers was ignored.

ACKNOWLEDGMENTS

The views expressed herein represent those of the authors not necessarily those of the sponsors. This project was sponsored by the Minnesota Department of Transportation and was supported in part by the University of Minnesota Supercomputing Institute.

REFERENCES

- AASHTO. 2004. *AASHTO LRFD Bridge Design Specifications, 3rd Edition*. Washington, DC: American Association of State Highway and Transportation Officials.
- Castrodale, R. W., A. Liu, and C.D. White. 2002. Simplified Analysis of Web Splitting in Pretensioned Concrete Girders. *Proceedings, 2002 Concrete Bridge Conference*, 1–18.
- Fountain, R.S. 1963. *A Field Inspection of Prestressed Concrete Bridges*. Portland Cement Association.
- Freyermuth, C.L. 1969. Design of Continuous Highway Bridges with Precast, Prestressed Concrete Girders. *Journal of the Prestressed Concrete Institute*, 14(2), 14–39.
- Gens, F., and J. Dotreppe. 2005. Neue formel für die berechnung von querzugspannungen in endbereichen von im sofortigen verbund vorgespannten tragern (A new formula for the calculation of transverse tensile stresses in end zones of pretensioned beams). *Betonwerk und Fertigteil-Technik (Concrete Precasting Plant and Technology)*, 71(1), 58–67.
- Gergely, P., M.A. Sozen, and C.P. Siess. 1963. *The Effect of Reinforcement on Anchorage Zone Cracks in Prestressed Concrete Members*. IHR-10. Urbana, IL.
- Marshall, W.T. and A.H. Mattock. 1962. Control of horizontal cracking in ends of pretensioned prestressed concrete girders. *Journal of the Prestressed Concrete Institute*, 7(5), 56–74.
- Miller, R.A., R. Castrodale, A. Mirmiran, and M. Hastak. 2004. *Connection of Simple-Span Precast Concrete Girders for Continuity*. NCHRP Report 519. Washington, DC: Transportation Research Board, National Research Council.
- Peterman, R.J., and J.A. Ramirez. 1998. Restraint Moments in Bridges with Full-Span Prestressed Concrete Form Panels. *PCI Journal*, 43(1), 54–73.
- Tuan, C. Y., S.A. Yehia, N. Jongpitaksseel, and M.K. Tadros. 2004. End Zone Reinforcement for Pretensioned Concrete Girders. *PCI Journal*, 49(3), 68–82.
- Tadros, M.K. and S.A. Yehia. 2003. *Prestressed Beam End Reinforcement and Camber*. NDOR Project Number SPR-PL-1 (38) P536. Lincoln, NE: University of Nebraska, Lincoln.